JOURNAL OF FORENSIC SCIENCES

J Forensic Sci, May 2011, Vol. 56, No. 3
doi: 10.1111/j.1556-4029.2010.01654.x
Available online at: onlinelibrary.wiley.com

PAPER

CRIMINALISTICS

Michael Colella,[1,2] *M.Sc.; Andrew Parkinson,*[1] *B.Sc.; Tegan Evans,*[1] *B.Sc.; J. Robertson,*[2] *Ph.D.; and Claude Roux,*[3] *Ph.D.*

The Effect of Ionizing Gamma Radiation on Natural and Synthetic Fibers and Its Implications for the Forensic Examination of Fiber Evidence*

ABSTRACT: Circumstances of criminal activities involving radioactive materials may mean fiber evidence recovered from a crime scene could have been exposed to materials emitting ionizing radiation. The consequences of radiation exposed fibers on the result of the forensic analysis and interpretation is explored. The effect of exposure to 1–1000 kGy radiation doses in natural and synthetic fibers was noticeable using comparative forensic examination methods, such as optical microscopy, microspectrophotometry, and thin-layer chromatography. Fourier transform infrared spectroscopy analysis showed no signs of radiation-induced chemical changes in any of the fiber structures. The outcome of the comparative methods highlights the risk of ''false negatives'' associated in comparing colors of recovered fibers that may have been exposed to unknown radiation doses. Consideration of such results supports the requirement to know the context, including the environmental conditions, as much as possible before undertaking a forensic fiber examination.

KEYWORDS: forensic science, radiologic forensics, fibers, fiber analysis techniques, ionizing radiation, CBRN forensics

Textile fibers transferred during an activity can be used as physical evidence in support of investigations or as evidence in court. For instance, an object left at a crime scene by a suspect may have fiber evidence that can link a suspect to the crime scene or in the very least provide investigative clues about the suspect's environment (1).

The importance of fibers as evidence will depend on a forensic scientist's ability to methodically examine and compare fibers collected from a crime scene with fibers collected from known sources, such as a suspect's garments, vehicle, or residence. Often, fiber examinations are complicated by the effects of environmental degradation of fibers (e.g., UV, heat, and moisture) and in some cases, the intentional alteration and destruction of all transient evidence by devious suspects (e.g., bleach, solvents) (1,2).

It is possible that in some circumstances fiber evidence recovered from what appeared to be a routine crime scene may have been exposed to materials emitting ionizing radiation. Unlikely as it may seem, criminal activities involving radioactive materials have been the center of attention for some time (3). Recent figures published by the International Atomic Energy Agency (IAEA) confirm there have been over 1340 incidents of nuclear materials trafficking and associated criminal activities investigated within the period of 1993 and 2007 (3). The IAEA believe that this figure represents a conservative estimate of the true figure, with growing concerns that more sophisticated and organized trafficking in nuclear materials may be occurring undetected. More concerning is that these incidents illustrate the potential threat of radioactive materials falling into the wrong hands (4,5). Given that the trafficking and illegal possession of radioactive materials constitute a breach of state or national law, a thorough criminal investigation into the circumstances of the situation will be warranted (6,7).

There have been extensive studies into the mechanisms for radiation damage (radiolysis) and in characterizing the performance of materials exposed to ionizing gamma radiation (8,9). Details regarding radiolytic mechanisms, such as the destruction of functional groups (e.g., carbonyl and carboxyl groups) and the formation of new molecules (e.g., chain scission, recombination, and cross-linkages), can be readily sourced from the literature (9).

Studies have mainly focused on the following aspects: assessing the performance of irradiated polymeric materials commonly used in the food packaging industry (10); characterizing the physiochemical and mechanical properties of polymers enhanced using radiolysis to catalyze chemical reactions; and assessing the stability of materials exposed to hard radiation environments often encountered in nuclear power plants, industrial irradiation facilities, and space crafts (11).

[1]Australian Nuclear Science & Technology Organisation, PMB 1, Menai, NSW 2234, Australia.
[2]Forensic and Technical Services, Australian Federal Police, Canberra, ACT 2611, Australia.
[3]Centre for Forensic Science, University of Technology Sydney, PO Box 123, Broadway, NSW 2007, Australia.

*Supported by the Australian Government Department of Prime Minister and Cabinet, the Australian Nuclear Science & Technology Organisation, and the Australian Federal Police (Contract: NSST 06-031).

Received 3 Dec. 2009; and in revised form 15 Feb. 2010; accepted 27 Feb. 2010.

© 2011 American Academy of Forensic Sciences

TABLE 1—*The properties for commonly used radioisotopes.*

Isotope	Activity Range	Common Use	Form	Half Life	Emissions
Cesium-137 (Cs-137)	37 GBq*–81.4 TBq†	Teletherapy, blood irradiations, and sterilization facilities	Solid; pressed powder	30.1 years	Beta and gamma radiation
Cobalt-60 (Co-60)	27 GBq–185 TBq	Teletherapy, industrial radiography, and sterilization facilities	Solid; metal	5.3 years	Beta and gamma radiation
Iridium-192 (Ir-192)	1200–2700 GBq	Industrial radiography and low-dose brachytherapy	Solid; metal	74 days	Beta and gamma radiation
Radium-226 (Ra-226)	3.7–370 GBq	Low-dose brachytherapy	Solid, metal	1600 years	Alpha and gamma radiation
Strontium-90 (Sr-90)	111 TBq–18.5 PBq‡	Radio-thermoelectric (RTG) generators	Solid, oxide powder	28.8 years	Beta radiation
Americium-241 (Am-241)	3.7–370 GBq	Well logging, thickness, moisture, and conveyor gauges	Solid, oxide powder	433 years	Alpha radiation
Plutonium-238 (Pu-238)	3.7–370 GBq	Heat sources for power generation (RTG)	Solid, oxide powder	88 years	Alpha radiation

*1 GBq = 1×10^6 Becquerels.
†1 TBq = 1×10^9 Becquerels.
‡1 PBq = 1×10^{12} Becquerels.

Radiation exposure (or absorbed dose) is generally measured using the standard international (SI) unit called the gray (Gy). The radiation exposure is equivalent to the energy "deposited" in a kilogram of a substance by the radiation. The important concept is that exposure is measured by what radiation does to substances, not anything particular about the radiation itself. This allows us to unify the measurement of different types of radiation (i.e., particles and wave) by measuring what they do to materials. As a point of reference, radiation exposures >6 Gy are almost certain to be fatal to humans (12).

In one study, paper substrates often used in manuscripts and books were irradiated and then characterized to ascertain if ionizing radiation could be effectively exploited in mitigating biodegradation in archival and historical material (13). Exposures to 14.4 kGy showed no discoloration or had any discernible impact on the mechanical properties of the paper substrates compared with artificially aged samples and the nonirradiated controls (13).

In a study into the effects of electron beam radiation on forensic evidence, writing inks on paper substrates were exposed to doses <30 kGy. The study reported a noticeable change in the UV fluorescence properties and a visible slight yellowing of the paper samples; however, the results suggested ionizing radiation had very little impact on the chemical analysis of writing inks (14). Similar studies at higher radiation exposures have shown significant radiation effects in document inks and dyes, and also in paper substrates. In particular, thin-layer chromatography revealed altered dye component mobilities and in one sample, the formation of a new dye component. It is likely that radiolysis of some of the organic constituents of the ink and paper substrate, combined with the elevated temperatures (from the electron irradiation process) contributed to these observed effects (15).

The present study focuses on radiation-induced deterioration of textile fibers and the potential impact of radiation-damaged fibers on the result of the forensic analysis. Of the few studies conducted examining the effects of ionizing radiation of physical evidence, most of the work has focussed on the electron beam irradiation processes (commonly used to biologically sanitize mail). As such, a variety of fibers were exposed to significantly higher radiation doses (compared to electron beam irradiators) to simulate exposures most likely to be encountered from commercial radioisotopes indentified in Table 1. Despite the fact that the radioisotopes indentified in Table 1 are generally considered to be hazardous, this study will focus on high activity radioisotopes (e.g., cesium-137, cobalt-60, and iridium-192) commonly used in industry (e.g., radiography, gauges) and in medicine (e.g., radiotherapy, blood irradiators).

The high total activity required for these applications and their widespread use in developed countries make these sources a significant security risk if they were used inappropriately or for malevolent intentions (e.g., radiologic dispersion device).

This study aims to assess the effects of ionizing radiation on a select choice of colored natural and synthetic textile fibers, including cotton, wool, acrylic, polyester, and nylon fibers. Conscious of the fact that a limited number of samples were used in this study, the intention of this work was to provide a representation of commonly found fiber samples and was not intended to be a population study.

Reported are a range of comparative forensic assessment techniques including optical microscopy, microspectrophotometry (MSP), Fourier transform infrared (FTIR) spectroscopy, and thin-layer chromatography (TLC) that were used to assess the major characteristics of the fibers (i.e., color, morphology) that were exposed to increasing doses of ionizing radiation.

Finally, this paper will attempt to establish whether or not ionizing radiation can compromise textile fiber evidence and if it is the case, is there a dose threshold where fiber evidence would still be exploitable?

Methods and Materials

Irradiation Parameters

To simulate realistic radiation exposures that forensic evidence might be subjected to in a variety of hypothetical scenarios, several key assumptions were established. These included the proximity of

TABLE 2—*Total radiation doses accumulated from hypothetical scenarios.*

Scenario	Source and Nominal Activity (GBq)	Time (h)	Total Dose (*c.* kGy)
Fiber evidence is situated 1 mm from the source	Ir-192 (2700 GBq)	24	7350
Fiber evidence is situated 1 mm from the source	Cs-137 (370 GBq)	168	4750
Fiber evidence is situated 10 mm from the source	Co-60 (185,000 GBq)	1	570

the evidence to the source, the exposure time, and the activity range for certain radioactive sources.

The premise for this research was that the sample fibers would be situated in close proximity (i.e., 1, 10, and 100 mm) from an unshielded source for a notional time period ranging from 24 h to 7 days. The third and most important parameter identified a number of radioactive sources commonly available in Australia that pose the greatest security risk (16,17).

TABLE 3—*Selection of fibers used in this study.*

Fiber Category	Brand and Origin	Color Details
Acrylic	Basics, China	Blue (048), Red (027), Black (113), and White (101)
Polyester	Gütermann, Germany	Blue (309), Red (156), Black (000), and White (800)
Nylon	Birch, China	Clear and Smokey
Pure Virgin Wool	DMC Laine Colbert Tapestry Wool, France	Blue, Red, Black, and White
Cotton	Gütermann, Greece	Blue (5123), Red (2074), Black (5201), and White (5709)

TABLE 4—*TLC extraction and elution methods.*

Fiber Type	Extraction Method	Elution Solvents
Acrylic fibers	Petrick et al. (12)	Ethyl acetate (CHEM Supply), absolute ethanol (CHEM Supply), and distilled water (70:35:30 v/v, respectively)
Wool fibers	Wiggens et al. (18)	*n*-propanol (CHEM Supply), methanol (CHEM Supply), deionized water, and ammonia (BDH ANALAR) (6:3:1:4 v/v respectively)
Cotton fibers	Wiggens et al. (18)	*n*-butanol (AJAX), ethanol (AJAX), ammonia (BDH), pyridine (CHEM Supply) and water (8:3:4:4:6 v/v respectively)
Polyester fibers	Petrick et al. (12)	Ethyl acetate (CHEM Supply), absolute ethanol (CHEM Supply), and distilled water (70:35:30 v/v, respectively)

The *a priori* absorbed dose values for the forensic samples calculated using the described parameters, ranged from 6.7 Gy to *c.* 11 MGy. However, careful analysis of the data suggested that the irradiation dose values ranging from 1 to 1000 kGy satisfactorily (and realistically) covered the majority of situations. It was determined that if the onset of radiation damage was not evident at 1000 kGy, then the likelihood of damage occurring would be negligible. Table 2 illustrates several hypothetical situations whereby transient textile fibers that have been exposed to industrial radioactive sources can accumulate significant radiation doses.

A MDS Nordion GammaCell (model 220 Excel) cobalt-60 research irradiator was used to simulate *in-situ* radiation exposure to the sample fibers. The irradiation exposure times (ranging from minutes to days) that are required to attain the appropriate doses were calculated via the use of simple mathematical relationships (12). Irradiation doses were measured and extrapolated using Harwell Perspex PMMA (batch 3042s) and Ceric-cerous (batch CCT) dosimeters. The ambient temperature in the irradiation chamber was *c.* 37°C.

Sample Preparation

The textile fiber yarn used in this study was sourced from domestic haberdashery and craft retail outlets and consisted of three synthetic yarns (polyester, acrylic, and nylon) and two natural yarns (cotton and wool). Specific characteristics of the sample yarns, including the manufacturer's details, are scheduled in Table 3.

Ten individual fibers, *c.* 5 cm in length from each of the different textile yarn samples, were collected to account for expected variations in both natural and to a lesser extent synthetic fibers. The fibers were prepared for irradiation by placing them in unbleached paper envelopes to minimize any potential radiolytic interaction of the envelope and the samples during the irradiation process. Because the irradiation process resulted in considerable damage in some samples and envelopes, the samples were carefully transferred to fresh light tight paper envelopes.

Optical Microscopy

Optical microscopy of the fiber samples was undertaken as a means to compare macroscopic properties of the irradiated fiber

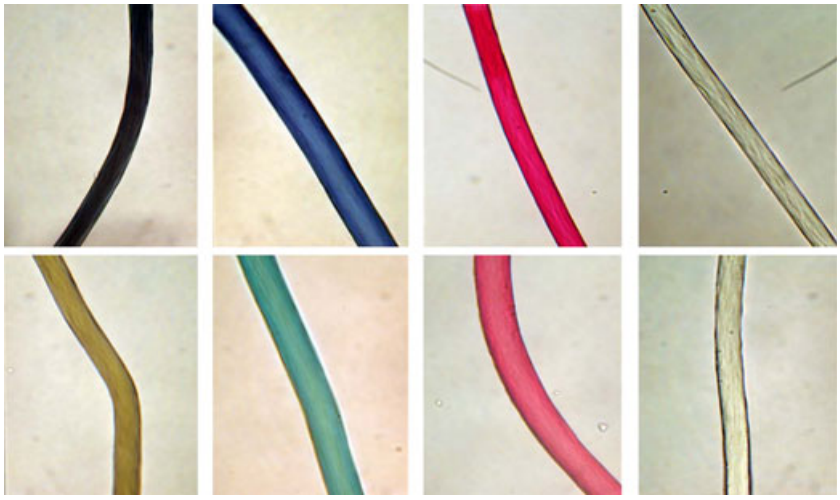

FIG. 1—*Micrographs of black, blue, red, and white colored acrylic fibers before irradiation (top); and the same acrylic fibers after 1000 kGy radiation exposure (bottom).*

samples to their respective control (0 kGy) fibers. Any changes to color, size, and the shape of the irradiated fibers that could perhaps infer radiation damage was noted and assessed.

Optical microscopy assessments were performed in triplicate. Fibers (*c.* 1 cm in length) were sampled from three different yarns for each category of fibers. The fibers were mounted onto a glass microscope slide using a dilute (50:50) glycerol–water solution (Chem-Supply, Port Adelaide, Australia) with a refractive index (RI) of 1.4007. Images were collected using a Leica DMR Fiber Comparison microscope integrated with a Canon Powershot G5 5.0 megapixel digital camera.

Microspectrophotometry

A SEE 2100 MSP (CRAIC Technologies, San Dimas, CA) integrated with proprietary spectral software was used to gather objective color information on the various fiber samples. Fiber samples were prepared and mounted for analysis using the same technique described previously for optical microscopy. MSP measurements were in transmission mode (15× objective magnification). The intensity (in % transmission) vs. wavelength (λ in nm) was measured between 380 and 880 nm, at 50 scans per measurement, using a 75W Xenon lamp (OSRAM, Munich, Germany).

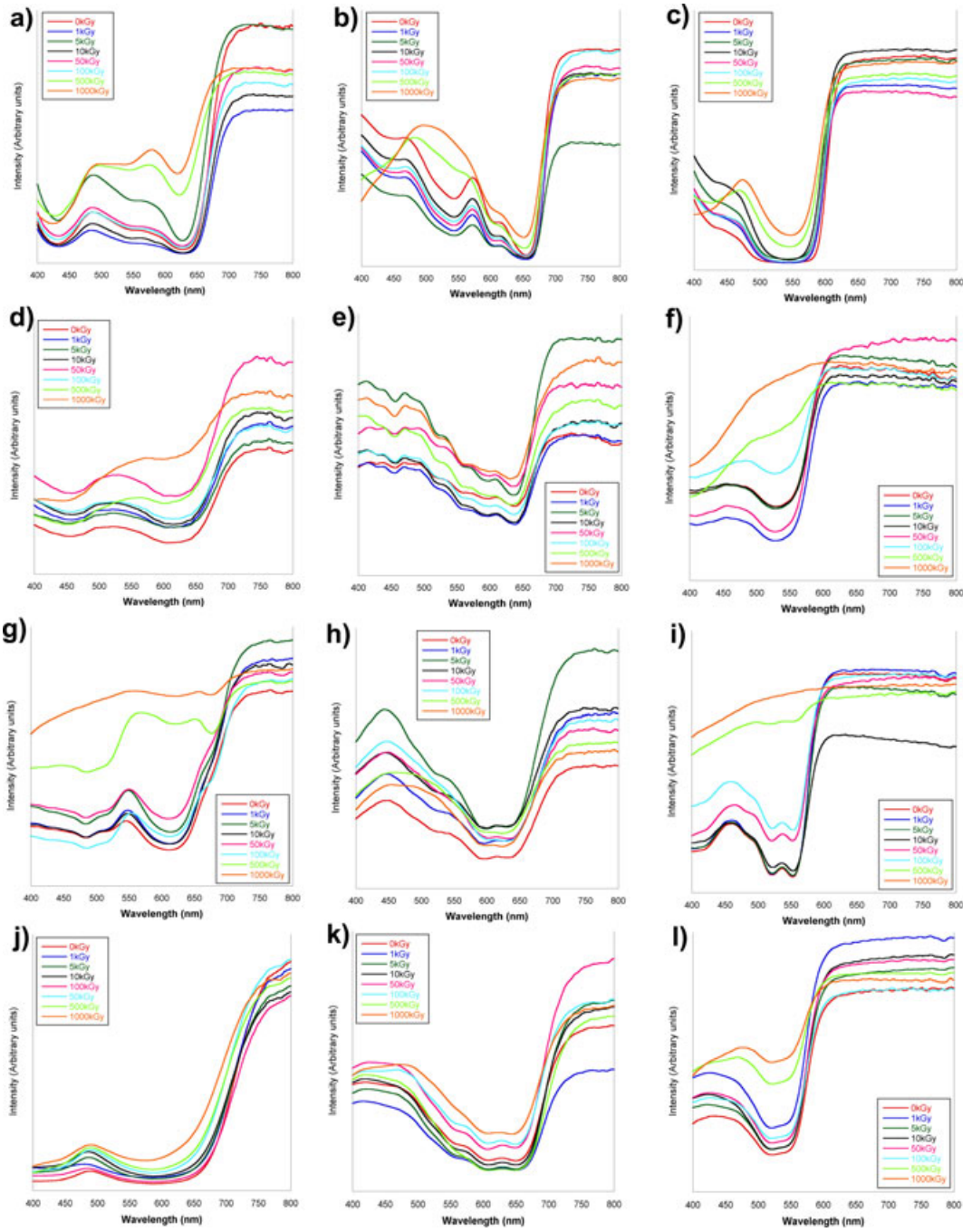

FIG. 2—*Microspectrophotometry graphs of (a) black, (b) blue, (c) red acrylic fibers; (d) black, (e) blue, (f) red polyester fibers; (g) black, (h) blue, (i) red cotton fibers; and (j) black, (k) blue, (l) red wool fibers exposed to increasing doses of radiation.*

A reference scan of the background (glass slide) was taken before collecting five sample scans at different positions along various samples, to account for inherent variations (e.g., nonhomogenous uptake of dyes; surface anomalies; thickness variation; and the presence of contaminants). Further treatment of the data with spectral software allowed the results to be presented in the form of average spectra.

FTIR Microspectrometry

FTIR is particularly well suited for obtaining unique molecular information on a microscopic scale from substrates, contaminants, and additives, which have distinctive functional groups including esters, carboxylic acids, amides, proteins, alcohols, and carbohydrates. Samples for each category of fiber were prepared for IR microscopy by cutting a 0.5 mm section from three individual fiber strands. The cut sections were carefully positioned in a SpectraTech diamond compression cell. The sections were placed under the infrared objective of a Thermo-Nicolet NicPlan® IR microscope (Thermo Fisher Scientific, Waltham, MA). The image was centered and the IR beam focused on the sample so that a transmission spectrum was obtained. A background spectrum was collected by focusing on just the diamond window.

All fiber samples were measured in triplicate and at a scan rate of 256 cycles and a 4/cm resolution. Spectra were afterward analyzed using Thermo-Nicolet OMNIC Custom Software v 7.1 (including Peak Resolve v7.0 and Spectral Interpretation Guide v1.0; Thermo Fisher Scientific) proprietary add-on software packages. To assist with data presentation, IR spectra were normalized to a common intensity scale using Kaleidagraph v4.6 (Synergy Software, Reading, PA), a commercial graphing and data analysis software package.

Thin-Layer Chromatography

Thin-layer chromatography (TLC) analyses of all the fibers used in this study were performed using Merck™ TLC silica gel 60 F_{254} plates (Darmstadt, Germany). The extraction and development methodology specific to each fiber type was adapted from various sources of literature (18,19). All dye samples were removed from the fiber substrate by cutting three 1 cm lengths of the fiber from three different fiber strands, followed by extraction with the appropriate solvents in micro vials (Agilent Technologies, Santa Clara, CA).

The extracted solutions were spotted onto the activated plate (activated by heating the TLC plate to 100°C for 10 min) using glass capillary tubes and allowed to air-dry to remove any residual extraction solvent. The nonirradiated dye sample (control) was spotted onto each plate as an internal reference standard. The spots were labelled 1 through 8 (from left to right: control to 1000 kGy). An individual lane (s) was also used to qualitatively determine any banding contributions by the solvent system. All the plates were eluted using mobile phases specific to the type of fiber. The mobile phases are identified in Table 4.

The developed plates were imaged and digitally recorded under white light and long wavelength UV light (350–650 nm). The TLC plate images were enhanced (i.e., brightness, color, contrast) using Adobe Photoshop image processing software to allow for more accurate measurements of the retention factor (R_f) values of the samples.

Results and Discussion

Acrylic

The effects of ionizing radiation in acrylic fiber samples were clearly evident using optical microscopy. Figure 1 shows progressive radiation damage to acrylic fibers. The black, blue, and red colored acrylic fibers showed considerable fading and color change. Fading in the colored acrylic fibers was apparent after a 5 kGy exposure, and the colorfastness progressively deteriorated with increasing dose.

MSP color spectra for acrylic fibers confirmed the optical microscopy observations. The MSP color profiles for black acrylic

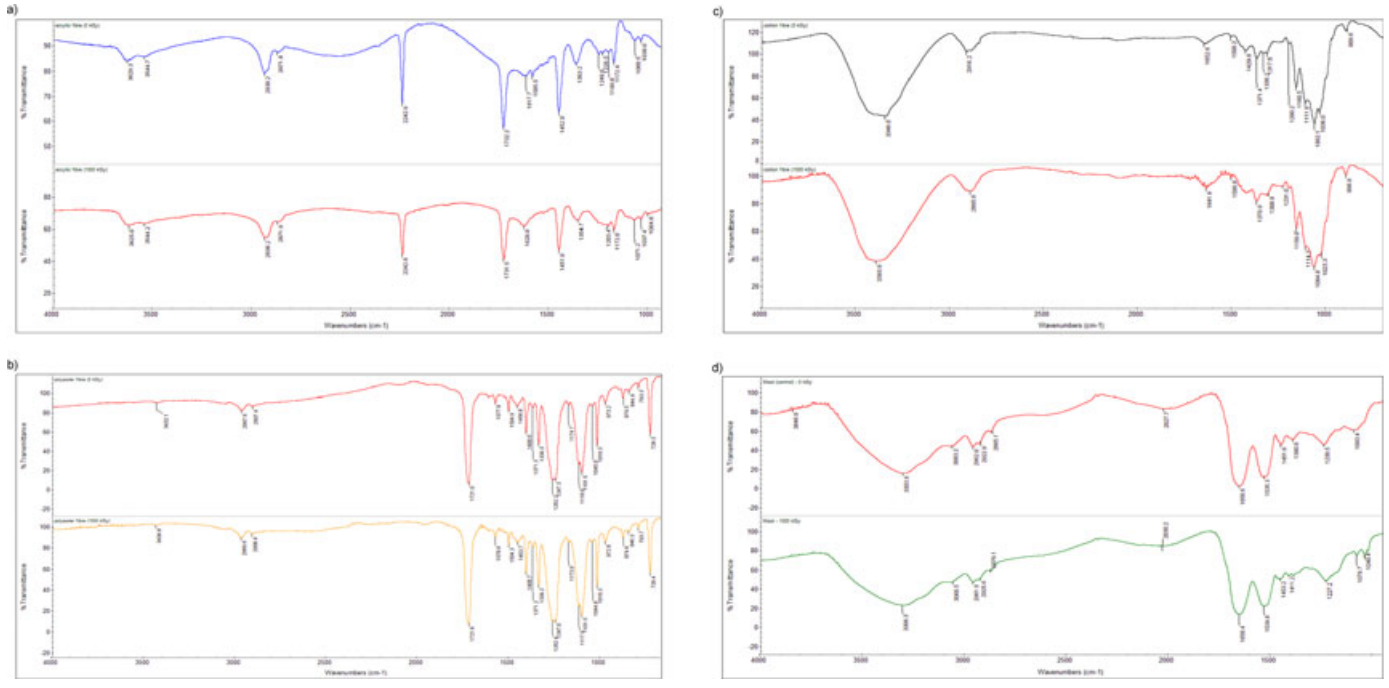

FIG. 3—*FTIR spectrum of (a) acrylic, (b) polyester, (c) cotton, and (d) wool fibers before irradiation (top); and after 1000 kGy radiation exposure (bottom).*

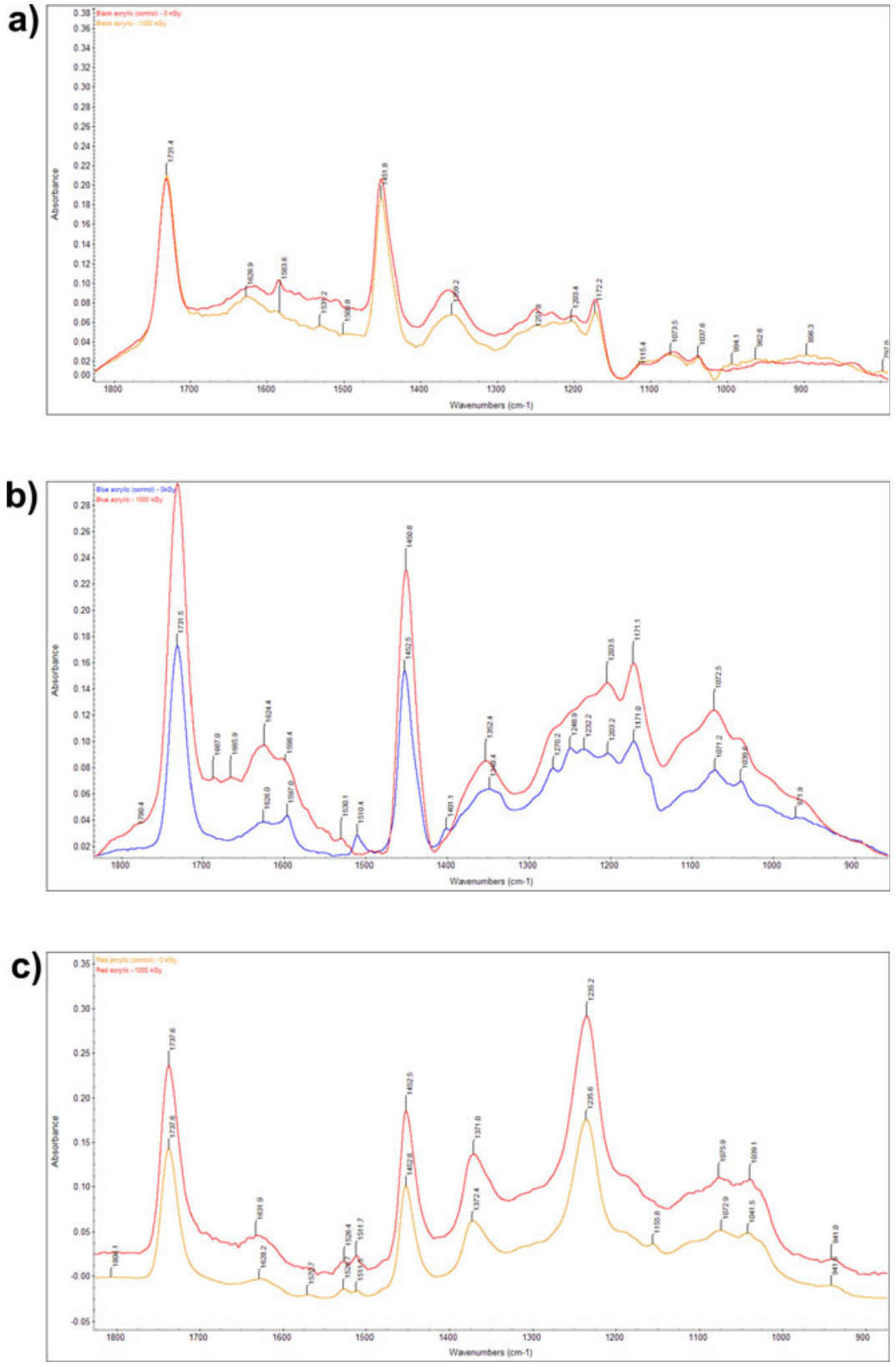

FIG. 4—*Comparative FTIR spectra of (a) black, (b) blue, and (c) red acrylic fibers before and after 1000 kGy irradiation.*

fiber (Fig. 2*a*) show a significant profile change occurring at exposures of 100 kGy and above, notably with the increasing intensity of the peak at *c.* 580 nm. Acrylic blue and red MSP spectra (Fig. 2*b,c*, respectively) show similar changes with increasing radiation. The prominent features in the blue acrylic fiber spectrum (a shoulder at *c.* 460 nm and a peak at *c.* 550 nm) clearly diminishes with dose and is subsequently incorporated into a broad rounded peak centered at *c.* 510 nm. In Fig. 2*c*, there is a gradual

increase in intensity and bathochromic peak shift from *c.* 455 to 460 nm. There were no noticeable changes in the MSP spectrum for the white acrylic fiber (figure not shown).

A possible explanation for the observed gradual changes in the colored acrylic MSP spectra is attributed to the ionization of pi (π) and sigma (σ) electrons in the conjugated aromatic chromophores, resulting in bond incisions and subsequent breakdown of the dyes.

TABLE 5—*TLC retention factors (R_f) for acrylic fibers.*

Control	1 kGy	5 kGy	10 kGy	50 kGy	100 kGy	500 kGy	1000 kGy
Retention factors (R_f) for black acrylic fiber							
Normal light							
0.65	0.65	0.64	0.63	0.62	0.62	0.63	0.64
0.47	0.47	0.47	0.46	0.46	0.46	0.46	0.46
0.45	0.45	0.45	0.44	0.44	0.44	0.44	0.44
0.42	0.42	0.42	0.41	0.41	0.41	0.41	0.41
0.40	0.40	0.40	0.39	0.39	0.39	0.39	0.39
450 nm							
0.65	0.65	0.64	0.63	0.62	0.62	0.63	0.64
0.47	0.47	0.47	0.46	0.46	0.46	0.46	0.46
0.42	0.42	0.42	0.41	0.41	0.41	0.41	0.41
–	–	–	–	–	–	0.18	0.18
–	–	–	–	–	–	0.11	0.11
Retention factors (R_f) for blue acrylic fiber							
Normal light							
0.45	0.45	0.45	0.45	0.45	0.45	0.45	0.46
0.38	0.38	0.38	0.38	0.38	0.38	0.38	0.39
0.35	0.35	0.35	0.35	0.35	0.35	0.35	0.35
450 nm							
–	–	–	–	–	–	0.78	0.78
–	–	–	–	–	–	0.62	0.64
–	–	–	–	–	–	0.55	0.56
0.45	0.45	0.45	0.45	0.45	0.45	0.45	0.45
–	–	–	–	0.38	0.38	0.39	0.39
0.35	0.35	0.35	0.35	0.35	0.35	0.35	0.35
Retention factors (R_f) for red acrylic fiber							
Normal light							
0.50	0.50	0.50	0.50	0.50	0.51	0.52	0.53
0.44	0.44	0.44	0.45	0.45	0.45	0.45	–
0.42	0.42	0.42	0.43	0.43	0.44	–	–
450 nm							
0.50	0.50	0.50	0.50	0.50	0.51	0.52	0.53
0.46	0.46	0.46	0.46	0.47	0.47	0.48	–

Figure 3*a* shows a representative FTIR spectrum within the mid-infrared region (4000 and 1000/cm) of acrylic fibers before and after exposure to 1000 kGy. The acrylic fiber used in this study was identified as polyacrylonitrile/methyl acrylate (PAN/MA) co-blend. All acrylic fibers show a major and intense peak at *c.* 2244/cm because of the –CN bond. The presence of the *c.* 1730/cm is indicative of the carbonyl group from the MA ester (1,20). Other major bands appear at *c.* 2930, 1450, and 1230/cm. These bands are all indicative of aliphatic functional groups, namely, CH_2 absorption band, CH_3 asymmetric deformation vibration, and the acrylate CO stretch. The presence of the same characteristic absorption bands after irradiation suggests that the polymer matrix of acrylic fibers is not damaged by relatively high radiation exposures.

Spectral characteristics of basic dyes, normally used as dispersive colorants in PAN/MA, are typically present between 1620 and 1520/cm (1). A closer examination of the spectral region between 1800 and 1000/cm was undertaken to assess whether any spectral variations could be attributed to radiation damage. The task was complicated by the fact that the basic dyes used are normally mixtures and the level of fiber dye is low, normally about 1–2% (19). Baseline corrected infrared absorbance spectra for black, blue, and red acrylic fibers before and after 1000 kGy irradiation are shown in Fig. 4.

Spectral features (shown in Fig. 4*a*) observed at *c.* 1586 and 1527/cm in the control (0 kGy samples) are attributed to a basic black mixed dye class. These features, along with several other undesignated basic dye peaks at *c.* 1551, 1500, 1483, and 1249/cm, fade with increasing radiation exposure (21). These peaks are no longer visible in fibers exposed to doses >100 kGy and compliment MSP and optical microscopy observations. Similar observations are noted in Fig. 4*b* (loss of bands at *c.* 1597, 1510, 1400 and 1270, 1249, and 1232/cm) and in Fig. 4*c* (loss of bands at *c.* 1570 and 1155/cm). These band assignments are associated with Basic Blue 41 (CI No. 11154) and Basic Red 27.

Thin-layer chromatograms for acrylic black, blue, and red dye extracts imaged in normal and UV (450 nm)/orange filtered lighting conditions (chromatograms not shown) were used to derive retention factor (R_f) values reported in Table 5. TLC analysis of the acrylic fibers showed slight discoloration (of the

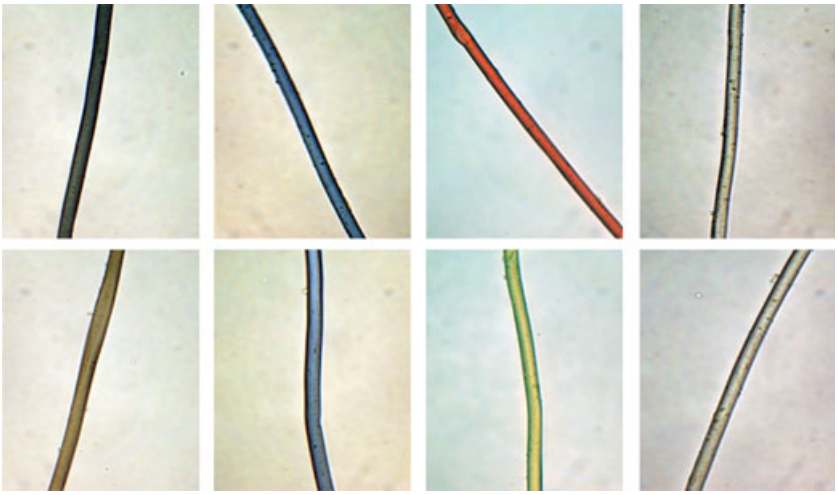

FIG. 5—*Micrographs of black, blue, red, and white colored polyester fibers before irradiation (top); and the same polyester fibers after 1000 kGy exposure (bottom).*

chromatograms) and band broadening in fibers exposed to doses >100 kGy. However, the calculated R_f values (shown in Table 5) suggest there were no significant changes in dye mobility (i.e., the bands and color separations were consistent with increasing radiation).

UV-filtered light chromatograms of the colored acrylics provided further insight. Although there were no signs of missing or new band gaps under normal light, UV-filtered light revealed some evidence of band broadening and the evolution of additional minor bands at high doses (100 and 500 kGy). In particular, the additional bands in black (R_f = 0.46 and 0.21), blue (R_f = 0.39 and 0.35), and red (R_f = 0.45 and 0.42) acrylic fibers were observed at doses greater that 100 kGy, which can possibly be attributed to radiolytic degradation of one or more of the chromophores present in the dyes, including additives such as optical brighteners.

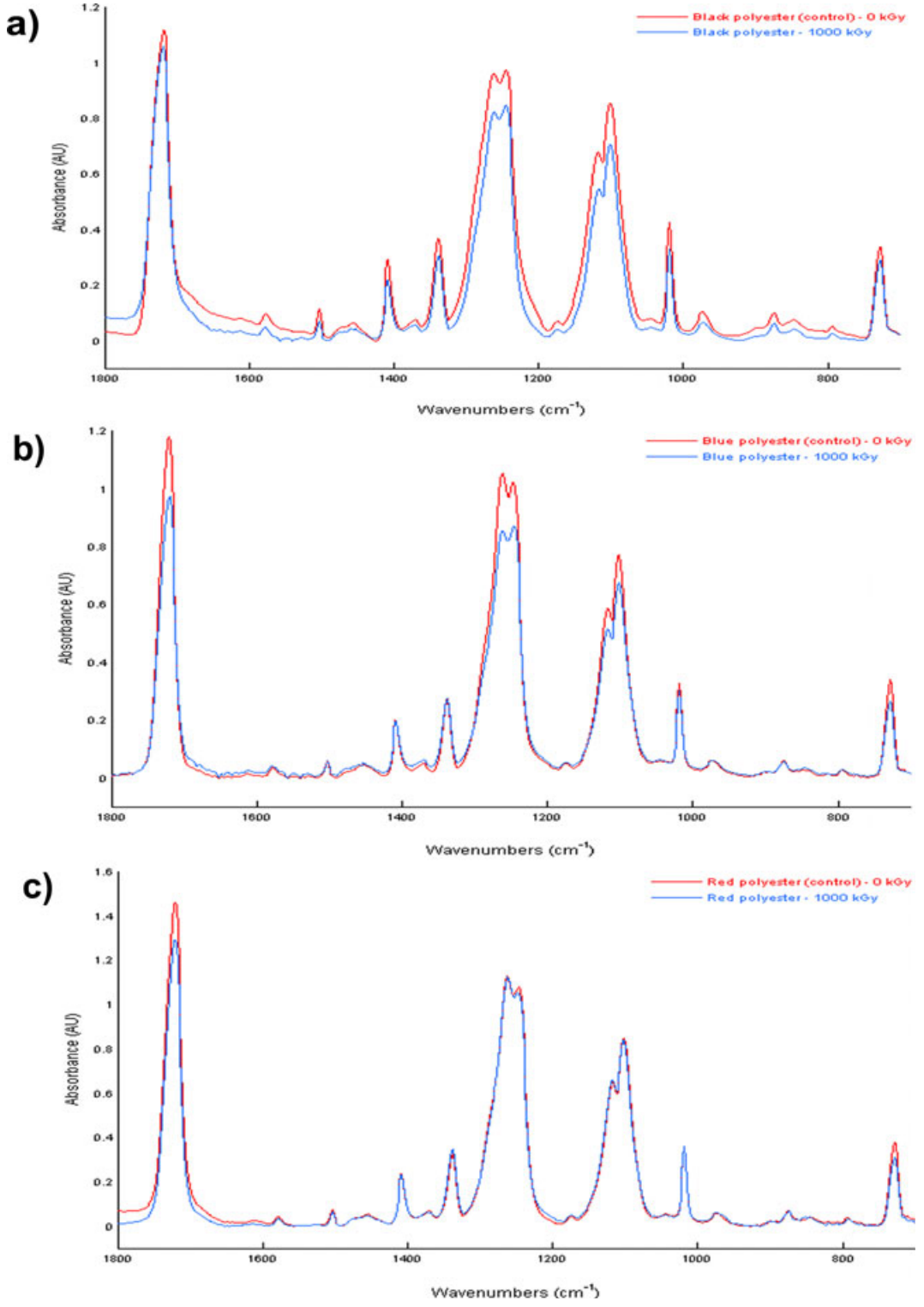

FIG. 6—*Comparative FTIR spectra of (a) black, (b) blue, and (c) red polyester fibers before and after 1000 kGy irradiation.*

Polyester

Comparative microscopy of black and red dispersive colored polyester fibers shown in Fig. 5 substantiates the progressive radiation damage (i.e., considerable fading and color change) with increasing ionizing radiation exposure. Fading in the black and red colored polyester fibers was apparent after 5 kGy exposure and progressively deteriorated with increasing dose. The blue colored fibers showed considerable resistivity to fading and discoloration.

TABLE 6—*TLC retention factors (R_f) for polyester fibers.*

Control	1 kGy	5 kGy	10 kGy	50 kGy	100 kGy	500 kGy	1000 kGy
Retention factors (R_f) for black polyester fiber							
Normal light							
0.87	0.87	0.87	0.87	0.87	0.87	0.87	0.87
0.84	0.84	0.84	0.84	0.84	0.84	0.84	0.84
0.80	0.80	0.80	0.80	0.80	0.80	0.80	0.80
450 nm							
–	–	–	–	–	–	0.85	0.85
–	–	–	–	–	–	0.78	0.78
–	–	–	–	–	–	0.65	0.65
–	–	–	–	–	–	0.50	0.50
Retention factors (R_f) for blue polyester fiber							
Normal light							
0.87	0.87	0.87	0.87	0.87	0.87	0.87	0.87
0.84	0.84	0.84	0.84	0.84	0.84	0.84	0.84
450 nm							
0.84	0.84	0.84	0.84	0.84	0.84	0.84	0.84
Retention factors (R_f) for red polyester fiber							
Normal light							
0.87	0.87	0.87	0.87	0.87	0.87	0.87	0.87
0.82	0.82	0.82	0.82	0.82	0.82	0.82	0.82
450 nm							
–	–	–	–	–	0.82	0.82	0.82
–	–	–	–	–	–	0.46	0.46
–	–	–	–	–	–	0.31	0.32
–	–	–	–	–	–	0.22	0.22

The MSP color spectra for black polyester fiber (Fig. 2*d*) show a gradual profile change occurring at exposures of 100 kGy and above, notably with the increasing intensity of the peak at *c.* 625 nm. The polyester red MSP spectrum (Fig. 2*f*) showed significant changes with increasing radiation. In particular, a prominent shoulder (*c.* 475 nm) and trough (*c.* 625 nm) clearly diminish with dose and is subsequently incorporated into a broad rounded peak centered at *c.* 525 nm. Noticeable changes were not present in the blue (Fig. 2*e*) and white polyester fibers (figure not shown) spectra.

Figure 3*b* shows a representative FTIR spectrum within the mid-infrared region (4000 and 1000/cm), for polyester fibers before and after exposure to 1000 kGy. All polyester fibers show a major and intense peak at *c.* 1720/cm corresponding to the conjugated C=O stretching vibrations (1,22).

Other major bands appear at *c.* 1420, 1240, 1100, and 1000/cm. These absorption bands are all indicative of the C-C stretching vibration in the aromatic ring, C-O-C unsymmetric and symmetric stretch of the ester, and C=C unsaturated stretch, respectively (23). The presence of the same characteristic absorption bands after irradiation suggests the polyester fibers (at first glance) are undamaged by relatively high radiation exposures. A closer examination of the spectral region between 1800 and 1000/cm was undertaken to assess whether any spectral variations in the main polyester absorbance peaks, or the spectral characteristics of dyes (typically present between 1620 and 1520/cm), could be attributed to radiation damage (23).

Previous studies suggested the stretching vibration of the aromatic ring (C-C; *c.* 1620/cm) to be radiolytically stable (21,24).

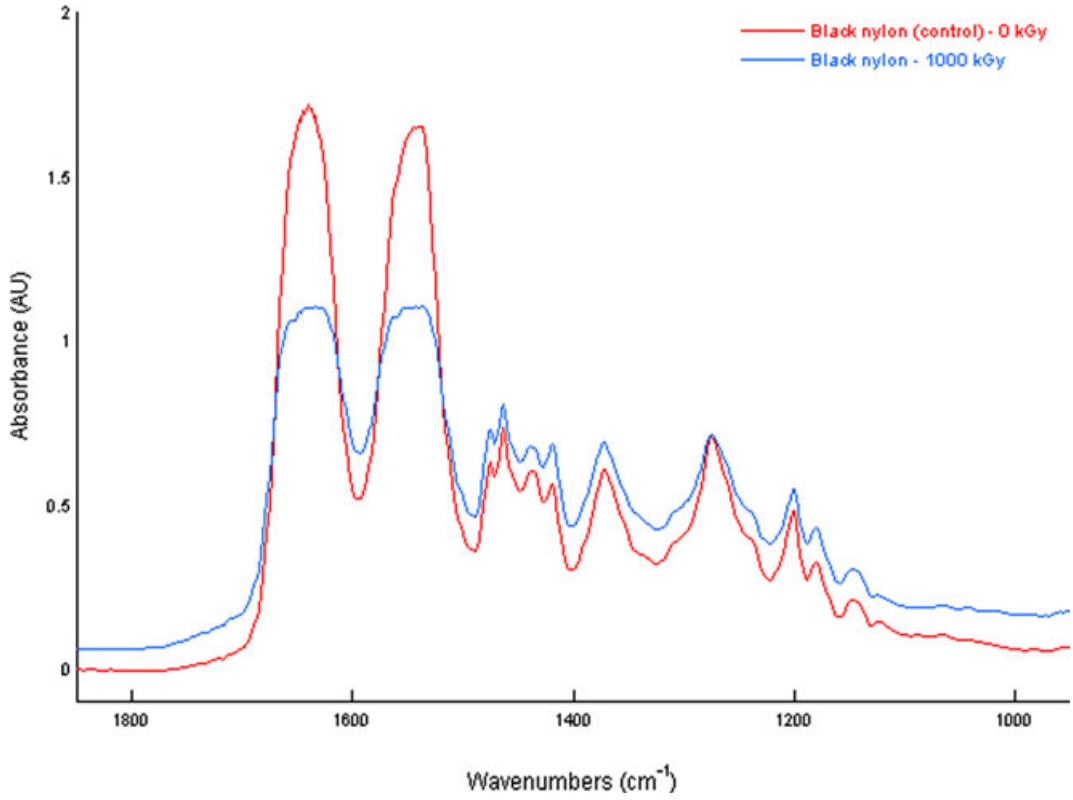

FIG. 7—*Comparative FTIR spectra of black nylon fiber before and after 1000 kGy irradiation.*

However, the other prominent absorbance bands (identified earlier) are reported to be affected by radiation. In particular, the carbonyl absorption (C=O; *c.* 1720/cm) peak increased with increasing radiation. This is most likely due to a break in the backbone of the molecule resulting in the formation of an alkoxyl radical and subsequent recombination with hydrogen to form R-COH (23). Baseline corrected infrared absorbance spectra for black, blue, and red polyester fibers before and after 1000 kGy irradiation are shown in Fig. 6.

Peak broadening in the C=O (*c.* 1720/cm) and O-C-O (*c.* 1240/cm) peaks observed in the baseline corrected IR spectra show some evidence of radiolytic damage. The relatively low concentration of dispersed dyes in polyester (similarly with acrylic dyes) made it problematic to determine the extent of radiolytic damage to the polyester dyes (1).

Retention factor (R_f) values for the colored polyester fiber dyes derived from the thin-layer chromatograms are reported in Table 6. TLC analysis for all the colored polyester dyes showed no significant changes in dye mobility. The calculated R_f values for black polyester dye were stable with increasing radiation. However, there was some evidence (particularly noticeable with filtered light) of band separation and discoloration at high doses (>100 kGy). Analysis of the blue polyester dye TLC also showed stability across the sample set. TLC analysis for red polyester showed significant changes with increasing radiation. The consistent R_f values (0.87 and 0.82) suggest no changes in the dye mobility; however, there was noticeable discoloration (under visible and UV lighting conditions) as expected at higher doses.

Nylon

The black (smokey) and clear fibers (images not presented) showed no evidence of discoloration or color fading with increasing radiation exposure. Although the relatively featureless MSP spectra (figures not shown) for both the clear and the black nylon fibers suggest there is no deterioration of the dye constituents, the fibers became very brittle and difficult to handle at higher doses.

Figure 7*a* shows a representative FTIR spectrum within the mid-infrared region of 4000 and 1000/cm, of Nylon 6-6 fiber before and after 1000 kGy. They show the typical polyamide bands at *c.* 3300/cm (N-H stretching), *c.* 1640/cm (C=O stretching; amide 1); *c.* 1540/cm (NH bending; amide 2) and *c.* 1467/cm (CH_2 bending). Other characteristic band assignments included the CH stretching bands at 2950 and 2850/cm, and at *c.* 1278/cm (C-N stretching and NH bending; amide 3), *c.* 1200/cm (NH wagging; amide 3), and *c.* 1150/cm (C-C stretching vibration) (24–26). There was no evidence of radiation damage, such as the formation of new peaks, existing peak broadening/splitting, or reduction in peaks that could be seen in the nylon infrared spectrum after exposure to high doses of radiation.

Figure 7*b* shows baseline corrected infrared absorbance spectra between the 1800 and 1000/cm spectral region of the fiber before and after 1000 kGy irradiation. No anomalies were identified in the infrared absorbance spectra, which could be attributed to the radiolytic decomposition of the black dye constituents.

TLC analysis for the black nylon fiber in visible and filtered light (results not shown) showed no changes in the dye mobility or missing bands or discoloration that might be attributed to radiation damage.

Cotton

The colored cotton fibers (shown in Fig. 8) displayed similar changes to those seen in the acrylic fibers. The onset of radiation damage (fading) was noticeable after 5 kGy and significantly progressed with increasing exposure. All the cotton fibers displayed very little color (appearing completely washed out) after being exposed to high radiation doses >500 kGy.

The progressive deterioration of the black and red colored cotton fibers (shown in Fig. 2*g*,*i*, respectively) was readily observed with MSP. The MSP spectra for both colored fibers significantly altered at 500 kGy and were relatively featureless at 1000 kGy (approaching what appeared to be a typical white MSP spectrum). The MSP spectrum for blue cotton fiber (Fig. 2*h*) also suggests some measure of radiation damage; however, MSP results were not consistent with optical microscopy. Upon close examination of the 1000 kGy blue cotton sample, residual coloring along the center axis of the fiber was evident. It is very likely that MSP data measurements were taken along the center axis, thereby influencing the MSP results from the expected typical white MSP spectrum. The white

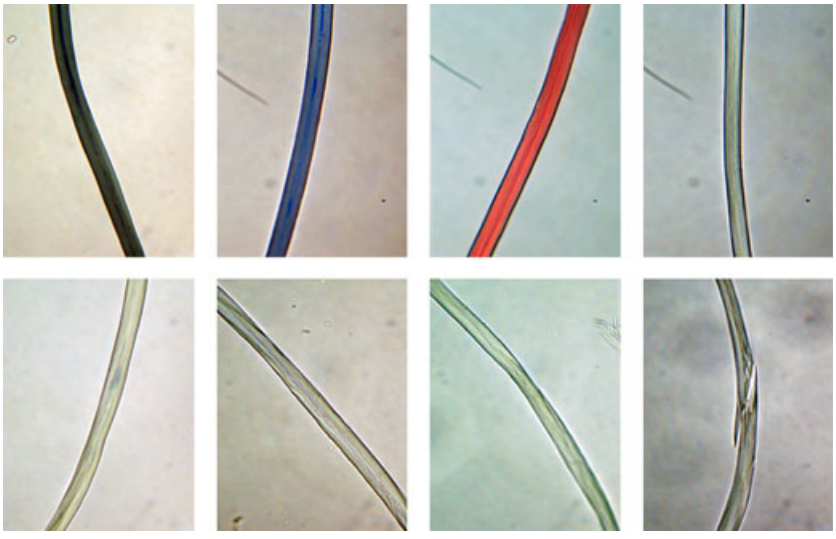

FIG. 8—*Micrographs of black, blue, red, and white colored cotton fibers before irradiation (top); and the same cotton fibers after 1000 kGy exposure (bottom).*

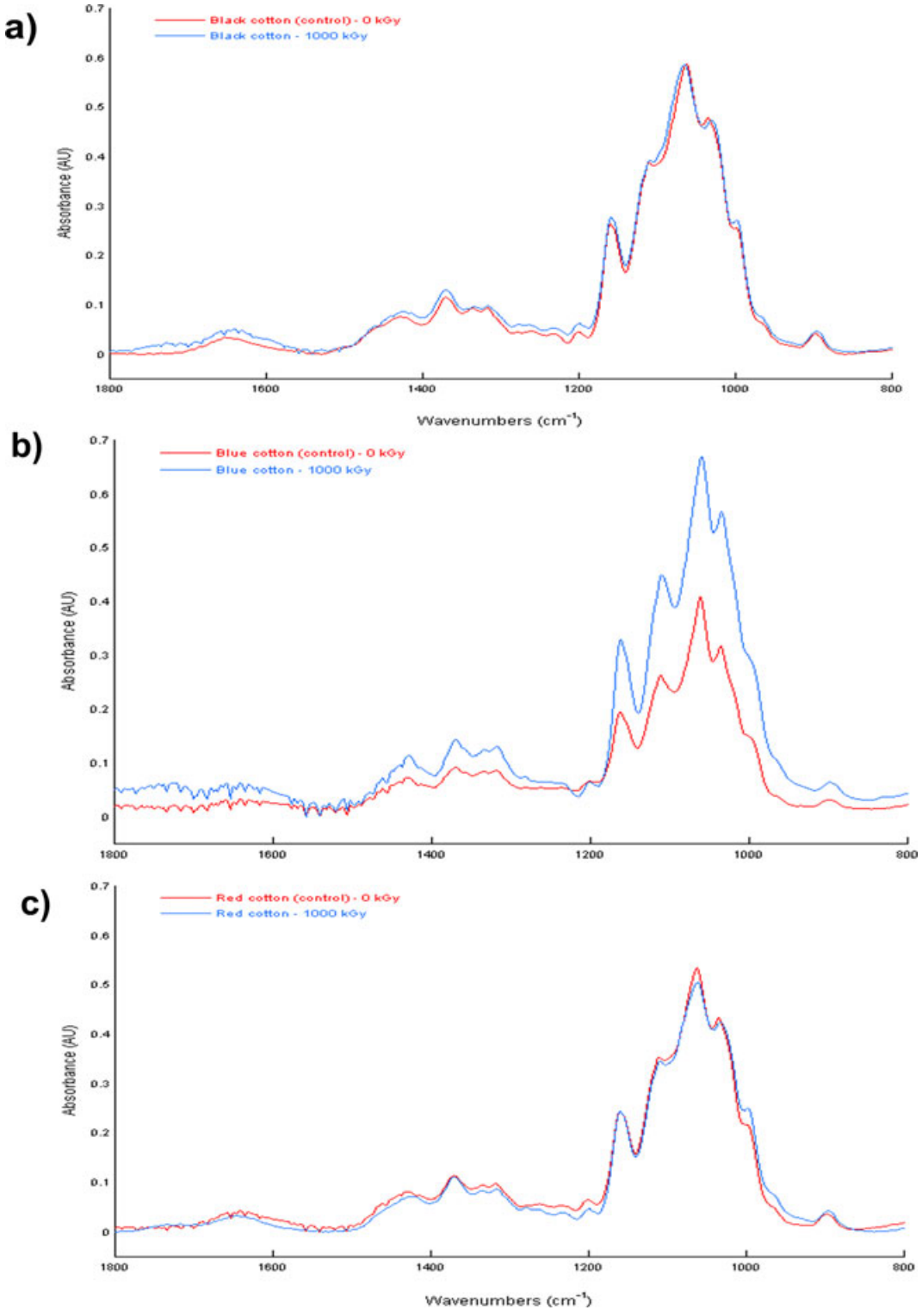

FIG. 9—*Comparative FTIR spectra of (a) black, (b) blue, and (c) red cotton fibers before and after 1000 kGy irradiation.*

color cotton spectra (figure not shown) indicated no discernible changes with increasing dose and appeared very similar to the 1000 kGy exposed cotton fibers.

Figure 3*c* shows a representative FTIR spectrum within the mid-infrared region (4000 and 1000/cm) of cotton fibers before and after 1000 kGy. Cotton fibers generally consist of predominantly 80–90% cellulose, 5% hemicelluloses and pectin, 5% water, with minor varying quantities of waxes, proteins, and ash (1,24). The major constituents account for the presence of characteristic bands at *c.* 3300 and 2900/cm because of polymeric OH (or hydroxyl associated with H-bonding) and C-H (1) asymmetric stretch, respectively (1). The modes in the 1800 to 1500/cm region are from the carboxylate anion (*c.* 1652/cm), as well as some overlapping involvements of C-H bending vibrations. The region below

1500/cm, the fingerprint region, is made up of additional bands that correlate mainly with carbohydrates and other bio-constituents, such as the CH_3 asymmetric deformation (*c.* 1370/cm) and the C=O and/or –OH deformation vibration (*c.* 1060/cm) (21). No evidence of radiation damage, such as the formation of new peaks, existing peak broadening/splitting or reduction in peaks, could be seen in the cotton infrared spectrum after exposure to high doses of radiation.

The spectral characteristics of dyes are typically present between 1620 and 1520/cm (22). A closer examination of the spectral region was undertaken to assess if any spectral variations could be attributed to radiation damage.

Baseline corrected infrared absorbance spectra for black, blue, and red cotton fibers before and after 1000 kGy irradiation (shown in Fig. 9*a–c*) suggested there were no discernible differences in the FTIR spectra, which conflicted with general MSP and optical microscopy observations. While the effects of ionizing radiation may not have manifested in chemical differences, it is likely that the shade differences observed using optical microscopy and MSP can be attributed to the radiolytic degradation of dyes.

Chromatograms for cotton black, blue, and red dye extracts imaged in normal and UV (450 nm)/orange filtered lighting conditions were used to derive retention factor (R_f) values reported in Table 7. TLC analysis of the colored cotton dyes showed no significant changes in dye mobility (with the exception of fiber dyes exposed to doses >100 kGy). At higher doses, evidence of discoloration, mobility changes (ΔR_f ranging from 0.03 to 0.06) and band loss were noted, and possibly attributed to radiolytic decomposition of the dyes. The missing R_f bands for the black (0.44 and 0.36), blue (0.50 and 0.37), and red (0.41 and 0.31) cotton dyes were evident under both lighting conditions for samples exposed to doses >100 kGy.

TABLE 7—*TLC retention factors (R_f) for cotton fibers.*

Control	1 kGy	5 kGy	10 kGy	50 kGy	100 kGy	500 kGy	1000 kGy
Retention factors (R_f) for black cotton fiber							
Normal light							
0.44	0.44	0.44	0.44	0.44	0.44	–	–
0.36	0.36	0.36	0.36	0.36	0.36	–	–
450 nm							
0.46	0.46	0.46	0.46	0.46	0.46	0.46	0.46
0.36	0.36	0.36	0.36	0.36	0.36	0.30	0.30
Retention factors (R_f) for blue cotton fiber							
Normal light							
0.49	0.50	0.50	0.50	0.50	0.50	–	–
0.34	0.37	0.37	0.37	0.37	0.37	–	–
450 nm							
0.33	0.34	0.34	0.34	0.34	0.34	0.34	0.34
0.36	0.37	0.37	0.37	0.37	0.37	0.31	0.31
Retention factors (R_f) for red cotton fiber							
Normal light							
0.41	0.41	0.41	0.41	0.41	0.41	–	–
0.32	0.31	0.31	0.31	0.31	0.31	–	–
450 nm							
0.43	0.43	0.43	0.43	0.43	0.43	0.43	0.43
0.31	0.31	0.30	0.30	0.30	0.29	0.27	0.27

Wool

The colored wool fibers (Fig. 10) were slightly affected by ionizing radiation. The onset of radiation damage (fading) varied from 10 to 50 kGy. High exposures (i.e., >500 kGy) appeared to significantly fade the red colored wool fibers, and to a lesser extent, the black and blue wool fibers.

The MSP spectra for the black and red colored fibers (Fig. 2*j*,*l*, respectively) show evidence of progressive radiation-induced damage with increasing exposure. In particular, the red wool fiber MSP spectra showed a significant change in profile, most notably an increase in intensity centered on the trough at *c.* 550 nm.

At higher doses, the MSP spectrum for the red wool fibers showed some similarities to that of the white wool fiber (figure not shown). The MSP spectrum of the blue wool fiber in Fig. 2*k* showed no evidence of degradation with increasing ionizing radiation.

Figure 3*d* shows a representative FTIR spectrum within the mid-infrared region of 4000 and 1000/cm, of wool fibers before and after 1000 kGy. The presence of characteristic bands at *c.* 3300 and 2900/cm because of polymeric OH (or hydroxyl associated with H=bonding) and C-H (1) asymmetric stretch, respectively, is associated with the major constituents of wool (i.e., keratin and cystine)

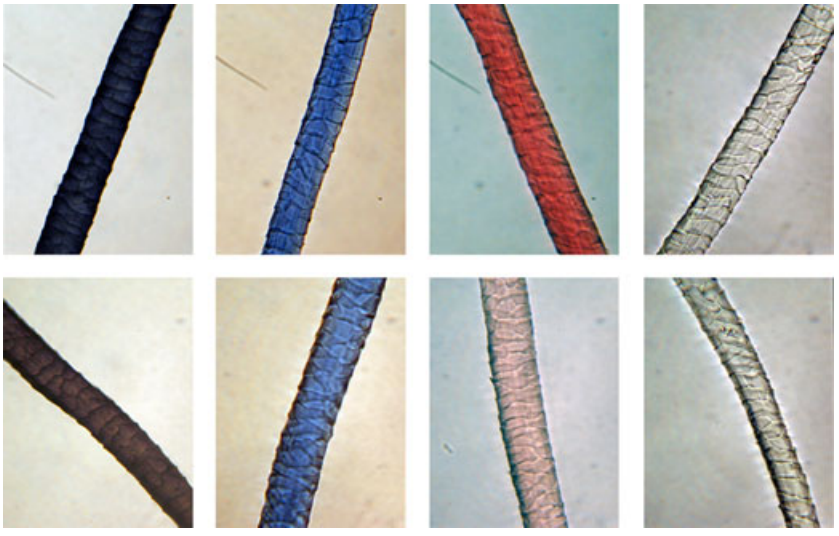

FIG. 10—*Micrographs of black, blue, red, and white colored wool fibers before irradiation (top); and the same wool fibers after 1000 kGy exposure (bottom).*

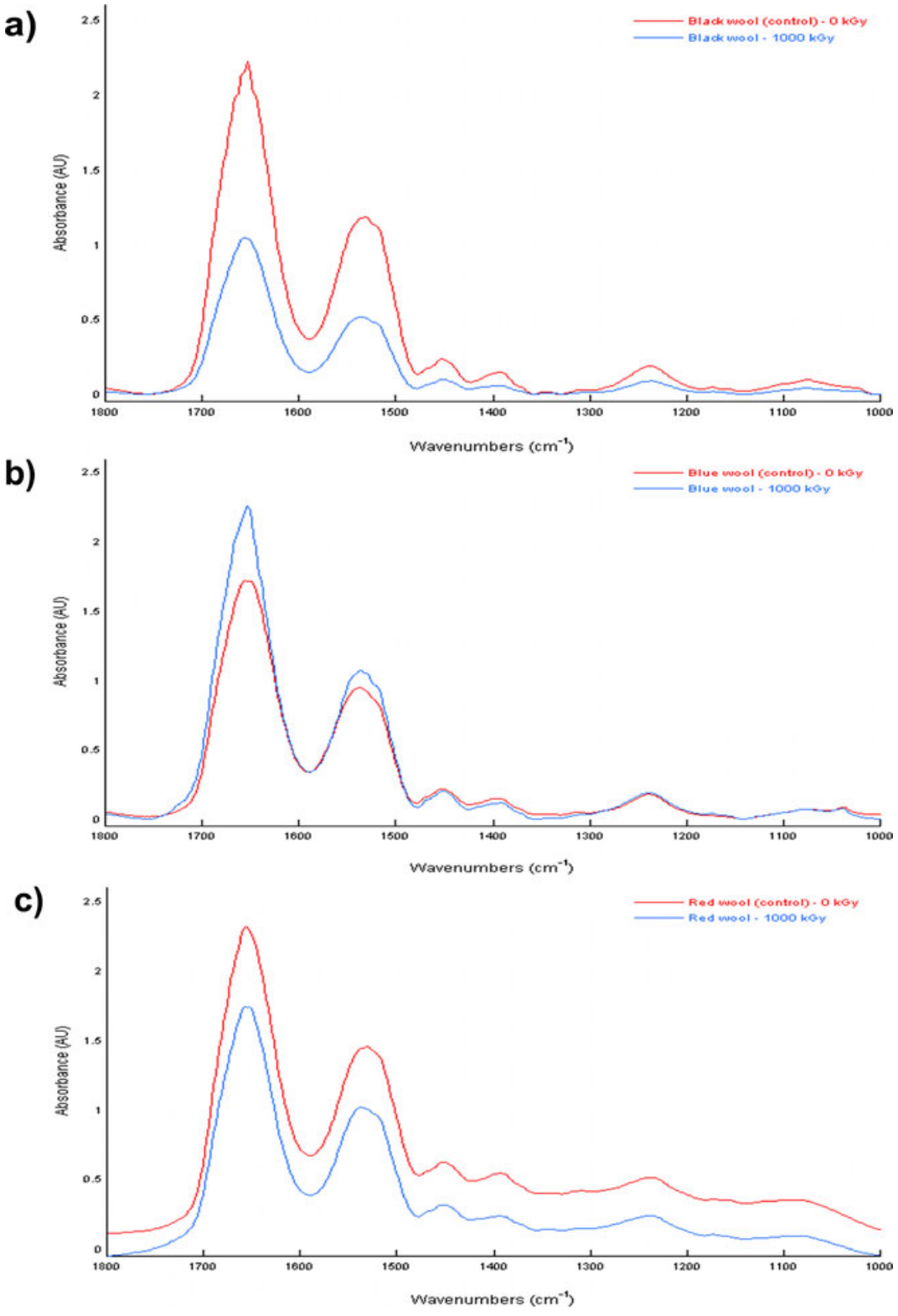

FIG. 11—*Comparative FTIR spectra of (a) black, (b) blue, and (c) red wool fibers before and after 1000 kGy irradiation.*

(1,28). A strong characteristic band at *c.* 1650/cm (amide 1) is attributed to the C=O stretch vibration indicative of the alpha helical structure. The amide 2 characteristic peak at *c.* 1538/cm corresponds to N-H bending and C-N stretching vibrations in the alpha helical structure. Amide 3 at *c.* 1230/cm corresponds to the in-phase combination of the C-N stretching and C=O bending vibrations (25,28). Similar to cotton fiber, the region below 1500/cm, the fingerprint region, is made up of additional bands that correlate mainly with carbohydrates and other bio-constituents, such as the CH_3 asymmetric deformation (*c.* 1370/cm) and the C=O and/or –OH deformation vibration (*c.* 1060/cm) (25,28). No evidence of radiation damage, such as the formation of new peaks, existing peak

TABLE 8—*TLC retention factors (R_f) for wool fibers.*

Control	1 kGy	5 kGy	10 kGy	50 kGy	100 kGy	500 kGy	1000 kGy
Retention factors (R_f) for black wool fiber							
Normal light							
0.86	0.86	0.86	0.89	0.89	0.89	0.89	0.89
0.83	0.83	0.83	0.83	0.83	0.83	0.83	0.83
0.73	0.73	0.73	0.73	0.73	0.73	0.73	0.73
0.69	0.69	0.69	0.69	0.69	0.69	0.69	0.69
450 nm							
0.80	0.80	0.80	0.81	0.81	0.81	0.81	0.81
0.71	0.71	0.71	0.71	0.71	0.71	0.71	0.71
0.66	0.66	0.69	0.69	0.69	0.69	0.69	0.67
Retention factors (R_f) for blue wool fiber							
Normal light							
0.86	0.87	0.87	0.87	0.87	0.87	0.87	0.87
0.71	0.73	0.73	0.73	0.73	0.73	0.73	0.73
0.64	0.67	0.69	0.69	0.69	0.69	0.69	0.69
0.41	0.43	0.43	0.43	0.43	0.43	0.43	0.43
450 nm							
0.63	0.66	0.66	0.66	0.66	0.66	0.66	0.66
0.41	0.43	0.43	0.43	0.43	0.43	0.43	0.43
Retention factors (R_f) for red wool fiber							
Normal light							
0.82	0.82	0.82	0.82	0.82	0.82	0.82	0.82
0.72	0.72	0.72	0.72	0.72	0.72	0.72	0.72
450 nm							
0.67	0.67	0.67	0.67	0.67	0.67	0.67	0.67

TABLE 9—*Summary of radiation damage observed in the fibers used in this study.*

Fiber Properties		Observed Radiation Damage			
Category	Color	Microscopy	MSP	FTIR	TLC
Acrylic	Black	Yes	Yes	–	Marginal
	Blue	Yes	Yes	Marginal	Marginal
	Red	Yes	Yes	–	Marginal
	White	–	–	–	–
Polyester	Black	–	Yes	–	–
	Blue	–	No	–	–
	Red	–	Yes	–	–
	White	–	–	–	–
Cotton	Black	Yes	Yes	–	Marginal
	Blue	Yes	Marginal	–	Marginal
	Red	Yes	Yes	–	Marginal
	White	–	–	–	–
Wool	Black	Marginal	No	–	–
	Blue	No	No	–	–
	Red	Yes	Yes	–	–
	White	–	–	–	–
Nylon	Smokey	–	–	–	–
	Clear	–	–	–	–

broadening/splitting or reduction in peaks could be seen in the wool infrared spectrum after exposure to high doses of radiation.

A closer examination of the 1800 and 1000/cm spectral region was undertaken to assess whether any variations could be attributed to radiation damage. Figure 11 shows baseline corrected infrared absorbance spectra for black, blue, and red wool fibers before and after 1000 kGy irradiation.

Previous studies have shown that the most significant changes (attributed to visible/UV radiation damage) occur in the amide 1 and amide 2 regions, indicating an increase in disordered structures and the possible formation of fatty acids from the oxidation of lipids in wool (23).

These observations were not evident in the wool IR absorbance spectra, suggesting that different radiation energies (i.e., UV photon radiation versus gamma [γ] radiation) may lead to different interaction mechanisms with the wool. Furthermore, no anomalies were identified in the infrared absorbance spectra, which could be attributed to the radiolytic decomposition of dyes. The most likely being due to the relatively low concentrations of basic dyes (*c.* 1–2%) used to color the wool fibers (20).

The TLC retention factor (R_f) values for the colored wool fiber dyes are reported in Table 8. TLC analysis for all the wool dyes (<100 kGy) in visible and filtered light showed no changes in the dye mobility or missing bands or discoloration that might be attributed to radiation damage. However, all the colored fibers showed varying levels of discoloration and fading (under both lighting conditions) at doses >100 kGy.

Conclusions

The effects of ionizing radiation in natural and synthetic fiber samples (summarized in Table 9) were noticeable using comparative forensic examination methods, such as optical microscopy, MSP, and thin-layer chromatography. In general, synthetic fibers showed early signs of progressive fading and some discoloration in radiation exposures >10 kGy. Natural fibers showed delayed onset of radiolytic damage at exposures >50 kGy, suggesting natural fibers were far more resilient to the ionizing radiation. This observation is consistent with radiation damage models in complex organic molecules. Generally, the excitation energy (i.e., ionizing gamma radiation) is transferred along the main C-C chain preventing chain scission. However, localized excitation in complex aromatic rings and functional groups (commonly found in dyes) will be far more susceptible to bond scission (18).

An assessment of radiolytic degradation of fibers and the dyes using FTIR analysis showed no signs of radiation-induced chemical changes in any of the fiber structures. The dye analysis, however, was inconclusive given that the dye concentration was typically <2% in weight and the inherently poor sensitivity of nonpolar molecules such as organic dye compounds resulted in a poor IR signal (21,29). Further work specifically assessing the extent of radiolytic degradation of dyes would perhaps benefit in using Raman spectroscopy, knowing that molecular vibrations from nonpolar organic molecules, such as organic dyes, are generally strong in the Raman spectrum.

Unfortunately, the onset of ionizing radiation damage is dependent on a range of variables (i.e., radioactive source, activity, distance, and time), which can manifest in just a few minutes' exposure.

The radiolytic degradation observed in this study is comparable to the chemical degradation of dyes influenced by environmental exposures such as sunlight (30). Although the incident photon energies are disparate between solar radiation (*c.* 10^{-19} joules; λ_{max} = 500 nm) and for Co-60 gamma radiation (*c.* 10^{-13} joules; Eγ = 1.3 MeV), the radiation damage mechanisms and subsequent degradation of the chromophore species are similar (9,30).

Nevertheless, apart from some marginal chemical changes and progressive color fading, forensic exploitation of recovered fiber evidence exposed to ionizing radiation is feasible, so long as there are allowances for progressive fading effects. However, the risk of "false negatives" associated in comparing colors of retrieved fibers that may have been subjected to dissimilar radiation exposures must be taken into account. These results support the need to know the context, including the environmental conditions, as much as possible before undertaking a forensic fiber examination.

Acknowledgments

The authors acknowledge the academic staff from the Centre for Forensic Science, University of Technology Sydney for their unwavering scientific and technical assistance throughout this study.

References

1. Roberston J, Grieve M. Forensic examination of fibres. In: Robertson J, editor. International forensic science and investigation series, 2nd edn. Boca Raton, FL: CRC Press, 1999;89–133.
2. Yinon J, Saar J. Analysis of dyes extracted from textile fibers by thermospray high-performance liquid chromatography-mass spectrometry. J Chromatogr A 1991;586:73–84.
3. International Atomic Energy Agency. IAEA Illicit Tracking Database (ITDB), Face Sheet (2008): 2, http://www.iaea.org/NewsCenter/Features/RadSources/PDF/fact_figures2007.pdf (accessed December 2009).
4. Schaper A. Nuclear smuggling in Europe real dangers and enigmatic deceptions. In: Kouzminov V, Martinelli M, editors. International forum. Illegal nuclear traffic: risks, safeguards and countermeasures; 1997 June; Como, Italy. Venice: UNESCO, 1997;4:125–44.
5. Webster WH, deBorchgrave A, Rupperman RH, Peterson E, Cilluffo FJ, Mullen SA, et al. The nuclear black market: global organised crime project. Washington, DC: Centre for Strategic and International Studies, CSIS Task Force Report, 1996.
6. Anzelon G, Hammond W, Nicholas M. The IAEA's illicit trafficking database programme. In: Proceedings of the International Conference on the Security of Materials: Measures to prevent, intercept and respond to illicit uses of nuclear material and radioactive sources; 2001 May 7–11; Sweden. Stockholm, Sweden: International Atomic Energy Agency (IAEA), 2001.
7. Drielak SC. Hot zone forensics. Chemical, biological, and radiological evidence collection. Illinois, USA: Charles C. Thomas Publisher Ltd., 2004.
8. Goulas AE, Riganokos KA, Kontominas MG. Effect of ionising radiation on physiochemical and mechanical properties of commercial monolayer and multilayer semigrid plastics packaging materials. Radiat Phys chem 2007;69:411–7.
9. Holmes-Siedle A, Adams L. Handbook of radiation effects, 2nd edn. Oxford, UK: Oxford University Press, 2006.
10. Komolprasert V, Diel T, Sadler G. Gamma irradiation of yellow and blue colorants in polystyrene packaging materials. Radiat Phys Chem 2006;75:149–60.
11. Davenas J, Stevenson I, Celette N, Cambon S, Gardette JL, Rivaton A, et al. Stability of polymers under ionising radiation interactions with polymers. Nucl Instrum Meth B 2002;191:653–61.
12. Martin A, Harbison SA. An introduction to radiation protection, 4th edn. New York, NY: Oxford University Press, 1996.
13. Magaudda G. The recovery of biodeteriorated books and archive documents through gamma radiation: some considerations on the results achieved. J Cult Herit 2004;5:113–8.
14. Ramotowski RS, Regen EM. Effect of electron beam irradiation on forensic evidence. 2. Analysis of writing inks on porous surfaces. J Forensic Sci 2007;52(3):604–9.
15. Solazzo C, Tumosa CS, Erdhardt D. The effect of electron beam irradiation on ballpoint pen and marker inks. MAAFS Newsl 2004;32(2): 13–6.
16. Colella M, Logan M, McIntosh S, Thomson SJ. An introduction to radiological terrorism. Aust J Emerg Manag 2005;20(2):9–17.
17. Ferguson CD, Kazi T, Perera J. Commercial radioactive sources; surveying the security risks. Occasional Paper No 11. Monterey, CA: Centre for Non Proliferation Studies, Monterey Institute of International Studies, 2003.
18. Petrick LM, Wilson TA, Fawcett WR. High performance liquid chromatography-ultraviolet-visible spectroscopy-electrospray ionization mass spectrometry method for acrylic and polyester forensic fiber dye analysis. J Forensic Sci 2006;51(4):771–9.
19. Wiggins KG, Holness J, March BM. The importance of thin layer chromatography and UV microspectrophotometry in the analysis of reactive dyes released from wool and cotton fibers. J Forensic Sci 2005;50(2): 364–8.
20. Grieve M. Another look at the classification of acrylic fibres, using FTIR microscopy. Sci Justice 1995;35(3):179–90.
21. Jochem G, Lehnert RJ. On the potential of Raman microscopy for the forensic analysis of coloured textile fibres. Sci Justice 2002;42(4):215–21.
22. Chae B, Woo Lee S, Ree M, Bin Kim S. Molecular orientation of new photosensitive polyesters for liquid crystal alignment. Vib Spectrosc 2002;870:1–4.
23. Pierpoint S, Silverman J, Al-Sheikhlyb M. Effects of ionizing radiation on the aging of polyester based polyurethane binder. Radiat Phys Chem 2001;62:163–9.
24. Allen A, Foulk J, Gamble G. Textile technology: preliminary Fourier-transform infrared spectroscopy analysis of cotton trash. J Cotton Sci 2007;11:68–74.
25. Zemaityte R, Jonaitiene V, Milasius R. Analysis and identification of fibre constitution of archaeological textiles. Mater Sci 2006;12(3):258–61.
26. Hendra PJ, Maddams WF, Royaud IA, Willis HA, Zichy V. The application of Fourier-transform Raman spectroscopy to the identification and characterisation of polyamides—1. Single number nylons. Spectrochim Acta A 1992;64(5):747–56.
27. Wang BB, Hu GS, Zhao X, Gao FZ. Preparation and characterisation of nylon 6 11 copolymer. Mater Lett 2006;60:2715–7.
28. Odlyha M, Theodorakopolous C, Campana R. Studies on woollen threads from historical tapestries. Autex Res J 2007;7(1):9–18.
29. Thomas J, Buzzini P, Massonnet G, Reedy B, Roux C. Raman spectroscopy and the forensic analysis of black/grey and blue cotton fibres. Part 1. Investigation of the effects of varying laser wavelength. Forensic Sci Int 2005;152:189–97.
30. Neppolian B, Choi HC, Sakthivel S, Arabindoo B, Murugesan V. Solar/UV-induced photocatalytic degradation of three commercial textile dyes. J Hazard Mater 2002;89:303–17.

Additional information and reprint requests:
Michael Colella, M.Sc.
Australian Nuclear Science & Technology Organisation
Private Mail Bag 1, Menai
NSW 2234, Australia
E-mail: michael.colella@ansto.gov.au